ΞSTiMatΞ

D2.1 Detailed reaction mechanism including PAHs, and soot
Version 0.1

Document Information

Contract Number	821418
Project Website	www.estimate-project.eu
Contractual Deadline	30.09.2021
Dissemination Level	Public
Nature	Report
Author	University of Stuttgart
Contributor(s)	-
Reviewer	-
Keywords	This deliverable describes the full reaction mechanism including precursors and PAHs and for kerosene-like fuel surrogates under the condition of interest for the project.

Change Log

Version	Author	Description of Change
V0.1		

Table of Contents

1.   Introduction

This deliverable describes the full reaction mechanism including precursors, PAHs and soot for kerosene-like fuel surrogates under the condition of interest for the project.

This deliverable describes the formulation and validation of the full detailed chemical kinetic reaction mechanism for a Jet A-1 surrogate at high temperature conditions. The development of detailed kinetics in this task is based on the surrogate fuel consisting of only a few components with well-known oxidation behaviour and with its characteristics being similar to Jet A-1 (fuel of interest). The reaction meodel developed was constructed according to the following protocol: (I) It is composed of many elementary reactions; (II) The combustion process is described starting from the reactants via the formation and decomposition of intermediate species up to the formation of the final combustion products, with main focus in PAHs (Polycyclic aromatic hydrocarbon) formation; (III) Each reaction scheme is characterised by a systematic and hierarchic structure; (IV) Selected fuel isomers interactions are considered by following the lumping approach, to allow for a more compact reaction scheme; (V) Reactions for low temperature conditions were not included; (VI) Both kinetic and thermodynamic parameters are provided. The mechanism developed in this task is called ESTiMatE-Mech.

The performance of the detailed reaction models constructed has been demonstrated with the help of selected relevant validation data. As such, species profiles, obtained within the oxidation of the Jet A-1 surrogate, surrogate components, and ethylene. These experimental data have been provided by the ESTiMatE partner KIT as a part of task T5.1 considering the experimental investigations of laminar counter-flow diffusion flames at atmospheric conditions. Further validation data was gathered from literature.

The mechanism developed is the starting point of the soot models that are included within the tasks of ESTiMatE partners TU Darmstadt, TU Eindhoven, and Barcelona Supercomputing Center (BSC): T2.4. Models for particle size distributions: EQMOM method lead by TU Darmstadt and T2.5. Models for particle size distributions: Sectional method lead by TU Eindhoven. Additionally, the mechanism generated will be part of the WP4 lead by BSC, with the assessment of the different models for the prediction of soot in practical applications being the main goal.

This deliverable is related with the deliverable D2.2: Chemical reaction mechanisms optimized for CFD applications. Deliverable D2.2 considers the reduction of the detailed reaction mechanism presented here (D2.1) thus enabling more efficient CFD calculations once incorporated.

2.   Mechanism development

In order to model Jet A-1 combustion, a detailed chemical kinetic mechanism is required. This is challenging due to its complex composition with up to hundreds of fuel species and the extensive chemical reaction network needed. Consequently, the combustion of Jet A-1 is modeled by means of a model fuel, also known as a surrogate; see e.g. [1-2]

and refs. therein. A jet fuel surrogate contains a few hydrocarbons selected from the different chemical families representing the major components and their fractions in a given kerosene. A surrogate can be designed such that it will have physical and chemical properties similar to those of the actual jet fuel. The following sections detail the different steps used to obtain an accurate and predictive model able to represent the chemistry involved in the combustion of Jet A-1: Surrogate formulation (section 2.1), mechanism development (sections 2.2 and 2.3), and mechanism validation (section 3).

2.1   Surrogate formulation

To obtain the optimal composition of the surrogate, the set of criteria must be specified for the optimization. In this case, these criteria are based on the chemical and physical properties of the target fuel, Jet A1. The targeted chemical and physical properties to optimize were: Combustion enthalpy, density of liquid, average molecular weight, viscosity, C/H ratio, sooting tendency index (defined by the threshold soot index -TSI), distillation curve, cetane number, and aromatic composition. The aromatic content was set to the maximal typical of the Jet A-1 following the objectives of the project to achieve a deeper understanding of the combustion of Jet A-1 and of the corresponding soot formation and destruction networks.

As a first step to define the surrogate composition, an approximation of the distribution of the different chemical families within a Jet A-1 was obtained from a gas chromatography (GCxGC) which allows to detect the type of family and the molecular weight distribution of the components within the real Jet A-1. At least one candidate for each typical chemical family was considered based on preliminary information from literature [3-6] and for the availability of the kinetic mechanisms for the species considered [7, 8]. For n-alkanes it was considered as possible candidates: n-decane and n-dodecane; for cycloalkanes: cyclohexane, methylcyclohexane and decalin; for iso-alkanes: iso-octane, and for aromatics: 1,3,5-trimethylbenzene, propylbenzene, toluene, and biphenyl. In the case of the aromatics it was dismissed any non-mono-aromatic because the GC analysis allows to identify that within the aromatics the higher proportion was mono-aromatics.

As a second step, a numerical optimizer based on a genetic algorithm has been implemented to assist the formulation of the fuel. The optimization of the composition of such a surrogate is a multi-target problem (number of targets to be matched defined as the number of physical and chemical properties considered) with multiple solutions. For the convergence of genetic algorithm were defined the following conditions: 500 for the number of possible combinations for the first population, 20 runs, 20 mutations for each run, and finally 10 for the number of the best compositions to mutate in the next round.

After the optimization process, several surrogates containing 4, 5, 6, and 7 species were formulated for Jet A-1. Targeting the use of the surrogate and corresponding kinetic mechanism in CFD modeling, the surrogate is desired to consider as limited number of

species as possible. For that reason, the 4 species surrogate was selected which included: n-dodecane 52%, iso-octane 15.8%, cyclohexane 12.1% and 1,3,5-trimethylbenzene 20.2%, all in volumetric fraction (Table 1). An important remark is given for the selection of 1.3,5-trimethylbenzene as the aromatic within the surrogate. 1,3,5-trimethylbenzene has been identified especially as the representative aromatic for the Jet A-1 surrogate that intends to mimic the Jet A-1 sooting tendency (high TSI index).

Table 1. Surrogate composition

Specie	Composition (volumetric fraction)
n-dodecane	52.0
Iso-octane	15.8
Cycloalkane	12.1
1,3,5-trimethylbenzene	20.2

2.2 Base mechanism

As a starting point for the development of the kinetic mechanism within ESTiMatE, a base mechanism was selected [7, 8]. This base reaction model [7, 8] contains all important molecular classes required for the detailed surrogate modeling of various fuels used in aviation and road transportation as well. It is a single reaction mechanism that includes reactions for the comprehensive description of the oxidation of many n-paraffins up to C_{16}, as well as iso-paraffins of varying degree of branching such as iso-octane (2,2,4-trimethyl-pentane), one methyl branched $iC_{11}H_{24}$ (2-methyl-decane), as well as $iC_{10}H_{22}$ (2,7 dimethyl-octane), and farnesane $iC_{15}H_{32}$ (2,6,10-trimethyl-dodecane); furthermore, cyclo-paraffins, e.g. cyclohexane, propylcyclohexane, and decalin, cyclo-aromatics, e.g. indane, indene, and tetralin, and aromatics, such as benzene, toluene, propylbenzene, styrene, naphthalene, methylnaphthalene, and biphenyl. All these hydrocarbons are validated as fuel compounds against data from various experimental setups. Over more, some higher PAHs up to C_{20} (e.g. phenanthrene, pyrene, chrysene) and polyynes up to C_{10} are implemented to represent a complete picture of soot precursors.

This base mechanism [7, 8] is modular and contains a wide range of components, not all of which are important to model the surrogate proposed within ESTiMatE. Therefore, some of them (larger iso-paraffins iC > 8 and larger n-alkanes nC > 12) were removed in order to keep only those components necessary to model the Jet A-1 surrogate. This compact version of the base mechanism includes 191 species and 1464 reactions.

The compact version of the base mechanism does not include, however the kinetics of one of the surrogate components: 1,3,5-trimethylbenzene. Therefore, a sub model for 1,3,5-trimethylbenzene needed to be developed and integrated into the base mechanism.

The resulting mechanism, after the incorporation of the new reaction paths and further modification of some of its reactions paths is called ESTiMatE-Mech.

2.3   Development and integration of the 1,3,5 – trimethylbenzene model

The development of a kinetic mechanism for 1,3,5-trimethylbenzene combustion implies as a first step the development of a reaction mechanism that can describe the m-xylene oxidation in a wide range of parameters. M-xylene is not only relevant because it is a major intermediate within the oxidation of trimethylbenzene, but also because the species produced by the initial hydrogen abstraction and decomposition reactions of 1,3,5-trimethylbenzene are mainly radical species that have been reported as major species within the m-xylene oxidation [9, 10]. After the integration of the m-xylene sub model to the base mechanism, the complete reaction paths for 1,3,5-trimethylbenzene can be developed and incorporated.

2.3.1   M-xylene sub model

A chemical kinetic reaction mechanism for the oxidation of m-xylene, consisting of 9 species and 62 reactions, has been developed and incorporated into the ESTiMatE-Mech. As a starting point to propose a new m-xylene sub model, different m-xylene mechanisms from literature [11-14] were analyzed by exploiting the rate of production (ROP) and sensitivity analysis to identify the reaction routes that are important to consider within m-xylene combustion.

The sub model proposed includes the initial unimolecular decomposition of m-xylene ($A_1CH_3CH_3$) to m-xylyl ($A_1CH_3CH_2$), the displacement reaction of one the methyl groups of m-xylene by an H-atom produces toluene (A_1CH_3) and the additionally thermal decomposition of m-xylene to produce m-methylphenyl radical ($C_6H_4CH_3$). Further reactions of m-xylene include the H-atom abstraction by different species yielding to m-xylyl (e.g. $A_1CH_3CH_3 + OH \leftrightharpoons A_1CH_3CH_2 + H_2O$).

The reaction pathway of $C_6H_4CH_3$ includes OA_1CH_3 which decomposes to A_1 (benzene) + CO + H as well as the reaction with H leading to toluene. The reactions of $A_1CH_3CH_2$ with O_2, O, OH, and HO_2 produce m-methylbenzaldehyde (A_1CH_3CHO). A second reaction path for m-xylyl radical, here reactions with O, H, and HO_2 forming $C_6H_4CH_3$, was also integrated. The A_1CH_3CHO produces by one route benzylic radicals with an aldehydic group (A_1CH_2CHO) and by a second route $C_6H_4CH_3$. Finally, A_1CH_2CHO reacts with O, O_2, OH, and HO_2 to form m-phthalaldehyde (m-$A_1CHOCHO$) which further produces benzaldehyde (A_1CHO). The termination path of benzaldehyde includes the formation of C_6H_5CO radical (which finally decomposes to A_{1-} + CO) and the decay to benzene. Figure 1 presents the reaction pathway for m-xylene combustion considered.

Experimental data from literature were considered to validate the m-xylene sub model: Ignition delay time from Battin-Leclerc et al. [15] and Shen and Oehlschlaeger [16], laminar burning velocity from Ji et al [17] and species concentration profiles from Gail and Dagaut [18]. Figures 2, 3 and 4 present the results for ignition delay time, laminar flame speed, and species concentration profiles, respectively. To outline some of the results calculated with ESTiMatE-Mech, they are compared with four mechanisms from literature [11-14]; only selected experimental conditions are given here, for more details, see [19].
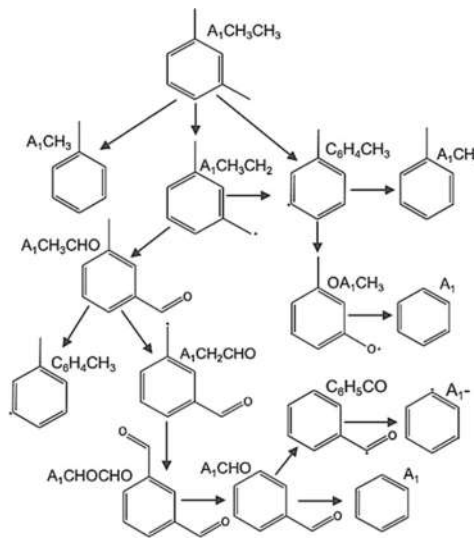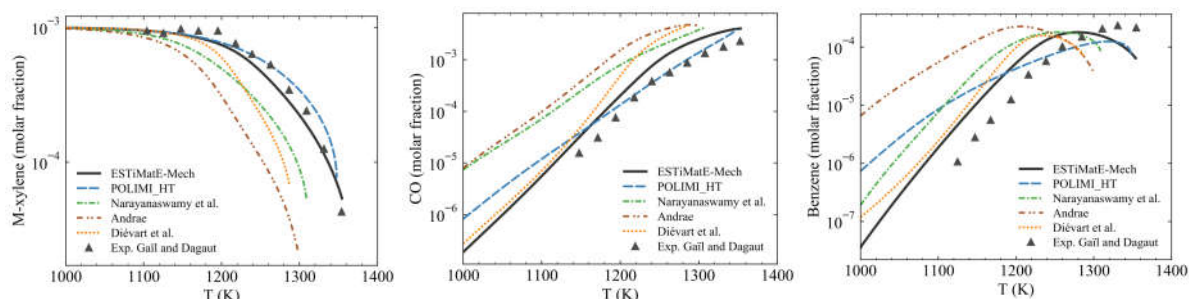
Fig. 1: Reaction pathway for m-xylene oxidation
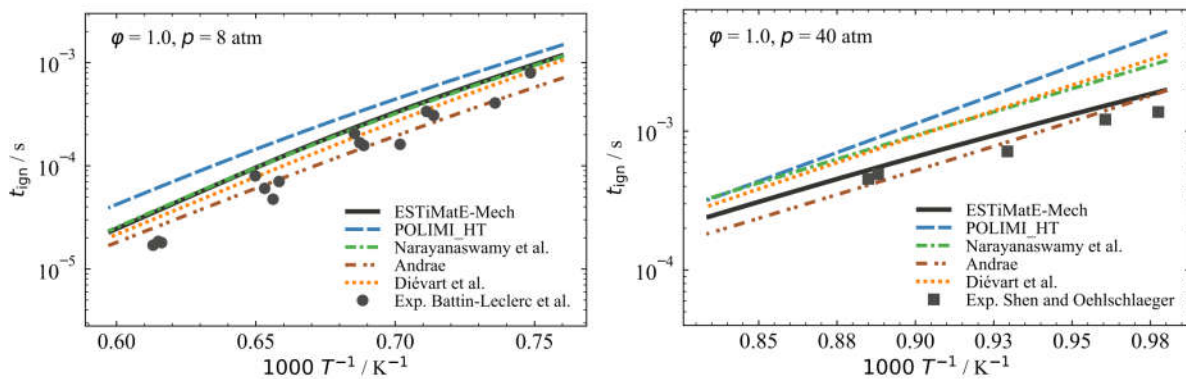
Fig. 2: Comparison between measured (symbols) and calculated ignition delay times (lines) of m-xylene at p = 8 and 40 atm [15,16].
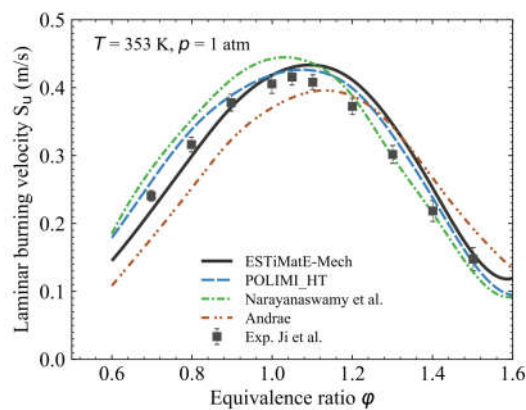
Fig. 3: Comparison between calculated laminar flame speeds of m-xylene/air mixtures with measured burning velocities from literature (symbols) [17]. T = 353 K, p = 1 atm.

Fig. 4: Comparison between calculated species concentration profiles (lines) and measured profiles in a jet stirred reactor [18] for m-xylene oxidation at p = 1 atm, φ =1.0 and a residence time of 0.1 s.

Overall, the presented m-xylene mechanism is a compact model that correctly predicts combustion properties of m-xylene. Ignition delay times at high pressures (up to 40 atm) and high temperatures (1020 K < T < 1680 K) can be accurately calculated for stoichiometric mixtures. ESTiMatE-Mech correctly predicts the laminar burning velocities of m-xylene/air mixtures at ambient pressure and different fuel equivalence ratios (lean, stoichiometric, and rich). Regarding species concentrations, the developed model predicts reasonably well the concentration of major and intermediate species at different temperatures and atmospheric pressure.

2.3.1 1,3,5 - Trimethylbenzene sub model

After the integration of the m-xylene model, a complete reaction path for 1,3,5-trimethylbenzene (1,3,5-TMB) was generated. This reaction path proposal is based fundamentally on well-known chemical kinetic mechanism of similar molecules, as the one from toluene and the previous developed m-xylene mechanism. Additionally, different detailed reaction mechanisms from literature [9,10,13, 14, 20], were analysed by rate of production (ROP) and sensitivity analysis to identify the most important reaction routes.

Figure 5 presents a basic scheme of the reaction pathways for 1,3,5-TMB combustion considered. The initial unimolecular decomposition of 1,3,5-TMB produces m-xylene ($A_1CH_3CH_3$), 3,5-dimethylbenzyl radical (RC_9H_{11}), and 3,5-dimethylphenyl radical ($C_6H_3(CH_3)_2$). The reaction pathway of $C_6H_3(CH_3)_2$ includes the dimethylphenoxy radical ($OC_6H_3(CH_3)_2$) which decomposes to A_1 (benzene) and toluene as well as the reaction with H leading to m-xylene. Further reactions of 1,3,5-TMB include the H-atom abstraction by different species yielding to RC_9H_{11} (e.g. 1,3,5-TMB + OH ⇋ RC_9H_{11} + H_2O). RC_9H_{11} produce the radical 35MBCH2O, 3,5-dimethylbenzaldehyd (35MBCHO), and methylxylylene (me2pxln). Additionally, from the mechanism developed by the CRECK modeling group for 1,2,4-trimethylbenzene [13, 14] was adapted the reaction: HO_2 +

$RC_9H_{11} \rightarrow OH + CH_2O + C_2H_4 + A_{1-}$. After the integration of the 1,3,5-TMB sub model to ESTiMatE-Mech, it was optimized with the linear transformation model (linTM) [21, 22] to increase the predictability of the experimental targets set for this work: laminar flame speeds and ignition delay times of 1,3,5-TMB. Here, the results of the optimized mechanism are presented.

Experimental data from literature were considered to validate the m-xylene sub model: Ignition delay time – from Diévart et al. [10] and Rao et al. [23], and laminar burning velocity – from Hui et al. [24] and Ji et al. [17]. Figure 6 and 7 present the results, with summarizing only selected experimental conditions.

Ignition delay times at high pressures and temperatures are accurately calculated with ESTiMatE_Mech as can be seen in Figure 6. Laminar burning velocities are also predicted correctly by ESTiMatE-Mech (Figure 7).
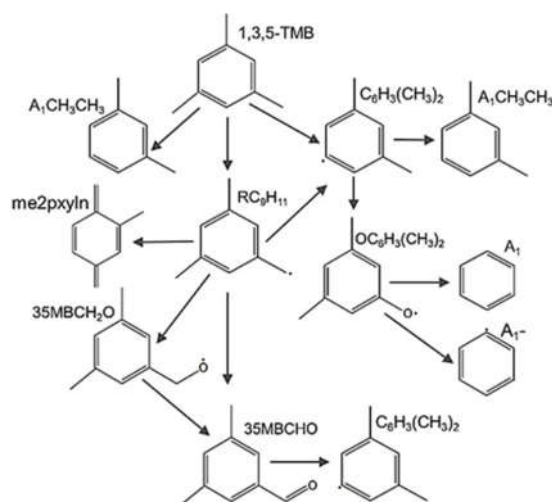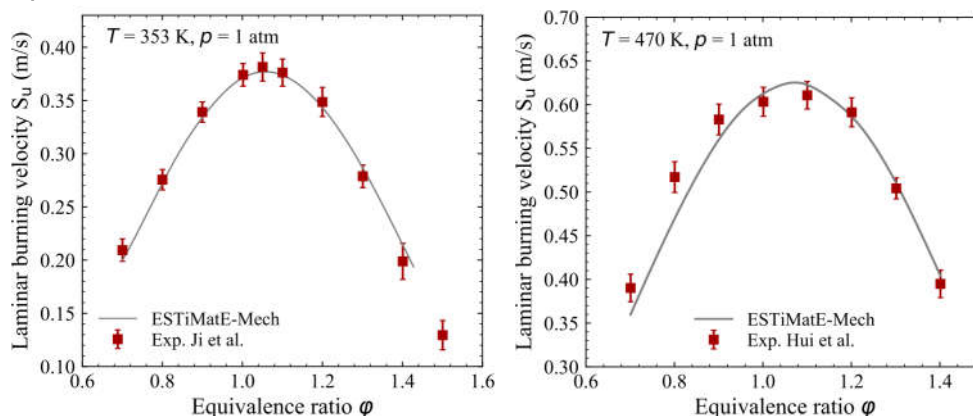

Fig. 5: Reaction pathways for 1,3,5-TMB oxidation.
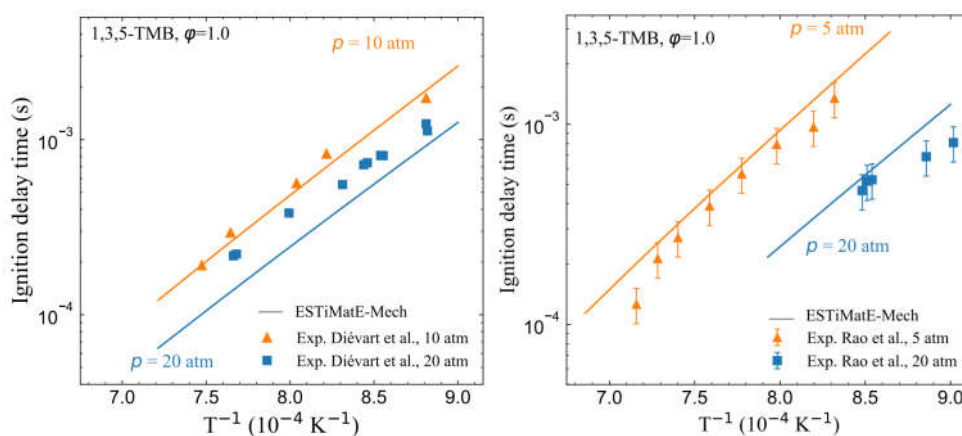
Fig. 6: Experimental [10, 23] and numerical results of ignition delay times of 1,3,5-TMB /

air flames, φ = 1.0.

Fig. 7: Experimental [17, 24] (symbols) and numerical (curves) laminar burning velocities of 1,3,5-TMB / air flames at 1 atm for two preheat temperatures, T = 353 and 470 K.

3. Mechanism validation

The performance of ESTiMatE-Mech was studied by comparison of calculated species concentration profiles with experimental ones for atmospheric non-premixed counterflow fuel-air flames provided by ESTiMatE partner KIT for iso-octane, ethylene and surrogate.

The counterflow flame data provided by ESTiMatE partner KIT has been simulated using Cantera [25], an open source code for the simulation of ideal chemical reactors. It computes the diffusion flame between two opposite burners solving for the temperature, species fractions, velocities and pressure gradients using a common set of governing equations within a 1D flow domain. The gas energy equation was solved accounting for the thermal radiation and the species diffusive mass fluxes are computed according to multicomponent formulation.

Initially, the ESTiMatE-Mech was validated for ethylene and iso-octane flames. The results with both fuels allow to identify the need to update the PAHs model within the mechanism to improve the prediction of the PAHs. In the following sub sections, the details about these results are presented.

After the validation with ethylene and iso-octane flames and the update of the mechanism to improve the prediction of the PAHs, the validation of the surrogate flames is presented.

### 3.1 Ethylene flames validation

Four ethylene flames were considered for validation of the ethylene sub model within the ESTiMatE-Mech. The experimental data for these flames was provided by the ESTiMatE partner KIT. These flames are:

- E-Y25-S60_s: Y_F = 0.25, α_2 = 60 s^{-1}. Sooting flame
- E-Y35-S60_s: Y_F = 0.35, α_2 = 60 s^{-1}. Sooting flame
- E-Y25-S100: Y_F = 0.25, α_2 = 100 s^{-1}. Non-sooting flame
- E-Y25_S120: Y_F = 0.25, α_2 = 120 s^{-1}. Non-sooting flame:
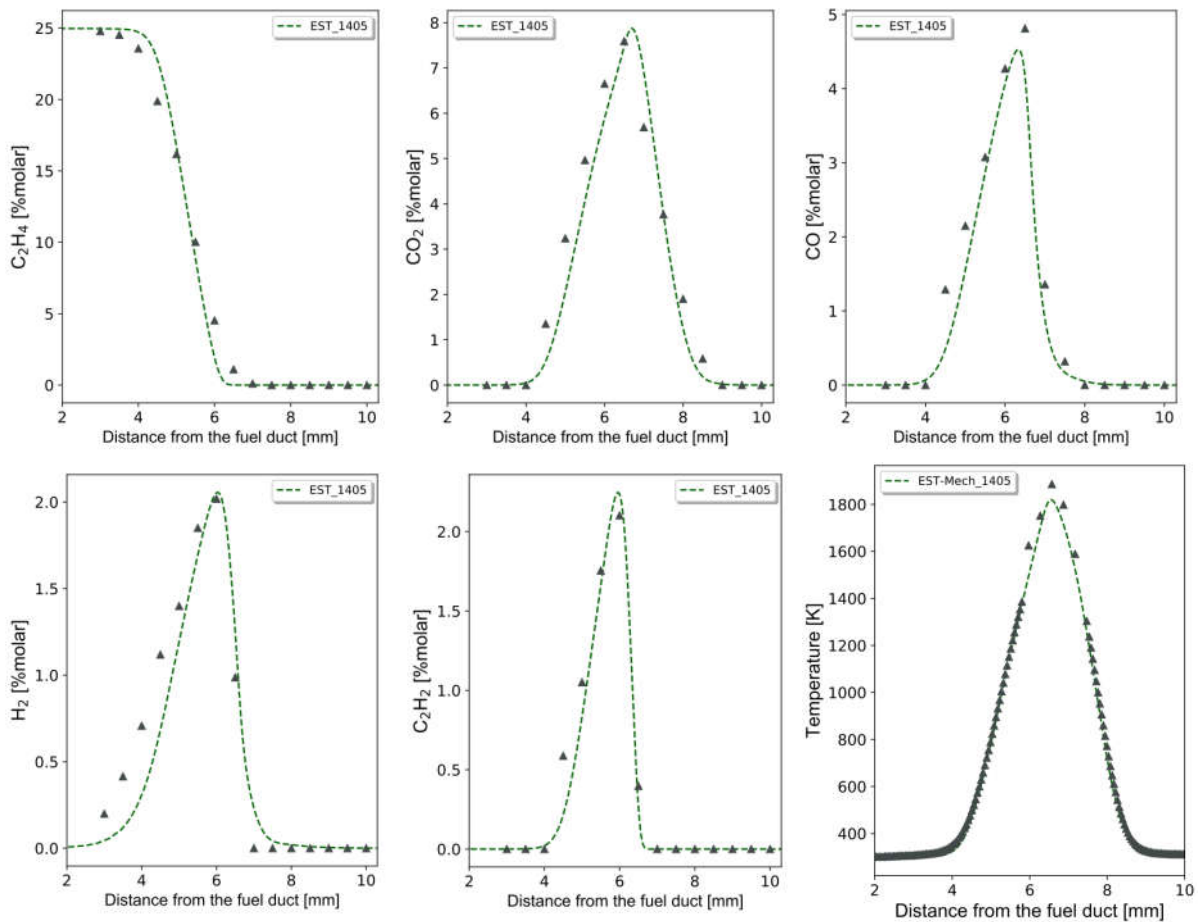
Fig. 8: Experimental (symbols) and numerical (curves) results obtained with ESTiMatE-Mech_1405 (EST-Mech_1405) of an ethylene counterflow flame: E-Y25_S100. Experimental results of the main species profiles and temperature profile.

The validation was carried out with a preliminary version of ESTiMatE-Mech. It was called ESTiMatE-Mech_14052021, which does not include any modification of the PAHs path already incorporated in the base mechanism. As an example of the modeling results of the counterflow flames, the results for one of the flames, here E-Y25_S100, are presented. As can be seen in Figure 8, with this mechanism version, a very good prediction of the main species profiles and temperature profile was achieved. However, Figure 9 shows that for that flame a considerable overprediction of the PAHs precursors: A1 (benzene), C_7H_8 (toluene), indene and naphthalene is observed. Additionally, for species that were not detected within the experiments: A3 (phenanthrene) and A4 (pyrene) because they were below the detection limits (about 1ppm), the concentrations observed within the simulation were considerably higher than the detection limits (Fig. 8).
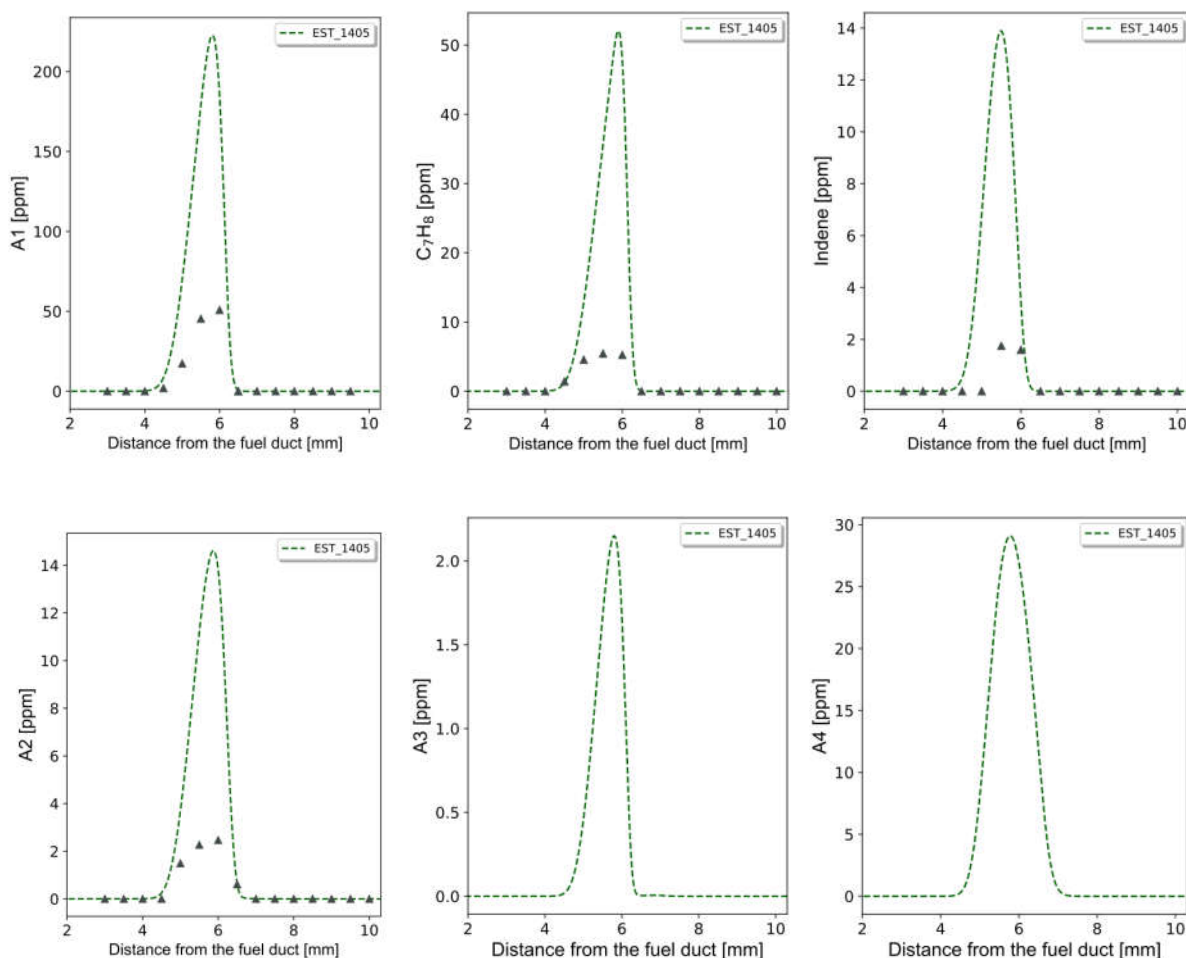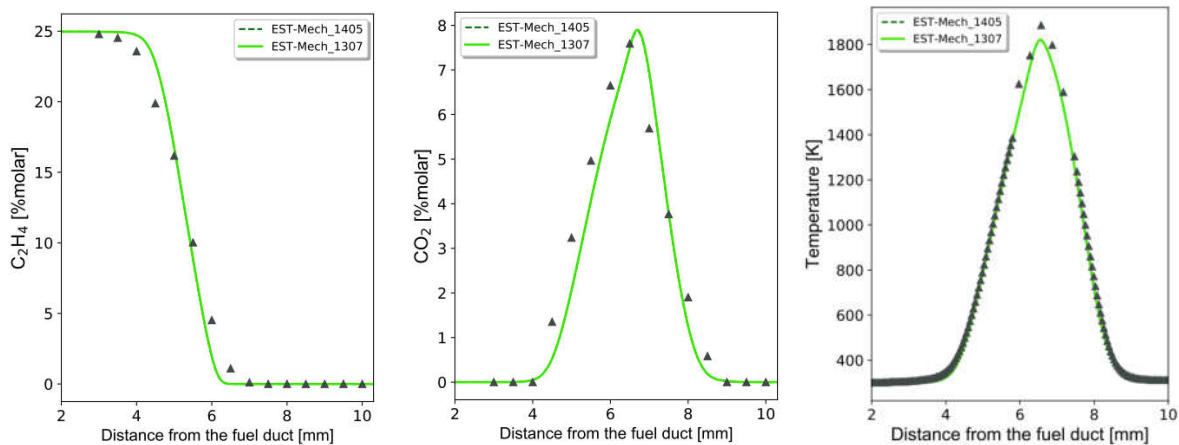
Fig. 9: Experimental (symbols) and numerical (curves) results obtained with ESTiMatE-Mech_1405 (EST-Mech_1405). of an ethylene counterflow flame: E-Y25_S100. Experimental results of the PAHs precursors and PAHs: A$_1$ (benzene), C$_7$H$_8$ (toluene), indene, A2 (naphthalene), A3 (phenanthrene), and A4 (pyrene).

For the four flames, the concentrations peaks of different species predicted by the simulations were compared with the concentration peaks from experimental data and plotted as % deviation at concentration peak. This plot is presented in Figure 10. This figure allows to show the considerable overprediction of the PAHs for all the flames.

Sensitivity analysis and rate of production analysis conducted to evaluate the role of reactions on the concentration profiles of the aromatic species. These analyses allow to identify the reactions path that were required to be modified or removed to have a better prediction of the PAHs precursors. After this process, a new version of the mechanism was proposed: ESTiMatE-Mech_13072021.
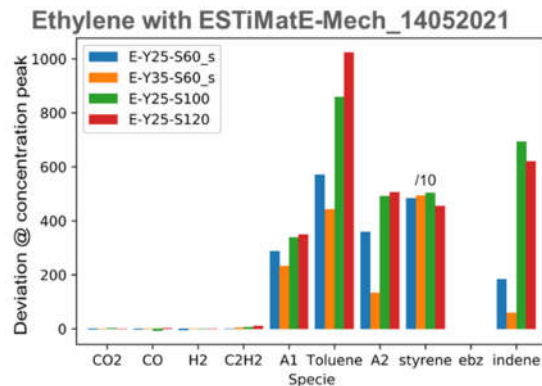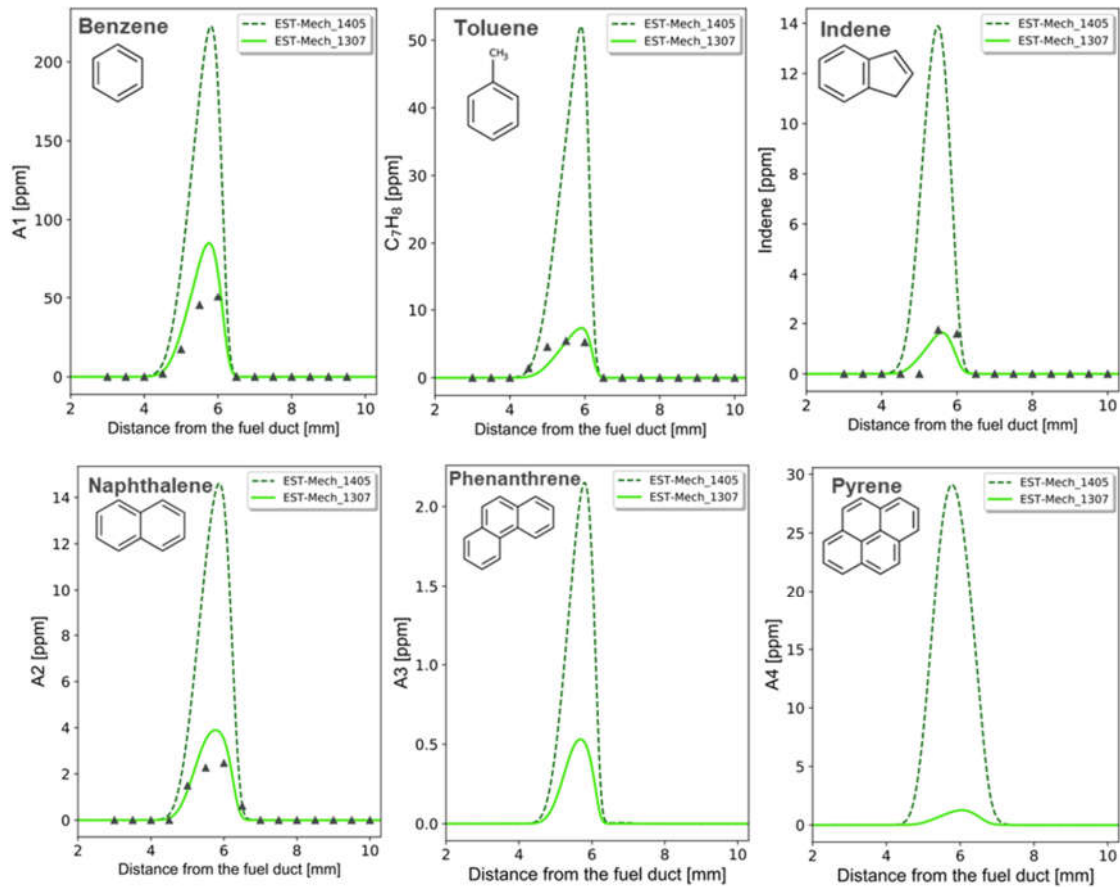
Fig. 10: Comparison between the concentrations peaks of different species predicted by the simulations with ESTiMatE-Mech_14052021 and the ones obtained from the experimental data


Fig. 11: Experimental (symbols) and numerical (curves) results obtained with ESTiMatE-Mech_1405 (EST-Mech_1405) and ESTiMatE-Mech_1307 (EST-Mech_1307) of an ethylene counterflow flame: E-Y25_S100 Experimental results of some the main species profiles and temperature profile.

The same ethylene counterflow flame (E-Y25-S100) was modeled to evaluate the difference between the two versions of the ESTiMatE-Mech: ESTiMatE-Mech_14052021 and ESTiMatE-Mech_13072021 (EST-Mech_1307). In this case both ESTiMatE-Mech-versions predict correctly main species and temperature profile as can be seen in Fig. 11.

ESTiMatE-Mech_1307 (EST-Mech_1307) improves considerably the predictions of the PAHs precursors as shown in the PAHs profiles presented in Figure 12. The prediction of the PAHs concentration profiles is considerably improved and the prediction of the PAHs for not detected species (A3, A4) is below the detection limits. Additionally, Figure 13 present that the % of deviation of the concentration peaks predicted by the simulations compared with the experiments is considerable reduced with ESTiMatE-Mech_1307.

Fig. 12: Experimental (symbols) and numerical (curves) results obtained with ESTiMatE-Mech_1405 (EST-Mech_1405) and ESTiMatE-Mech_1307 (EST-Mech_1307) of an ethylene counterflow flame: E-Y25_S100 Experimental results of the PAHs.
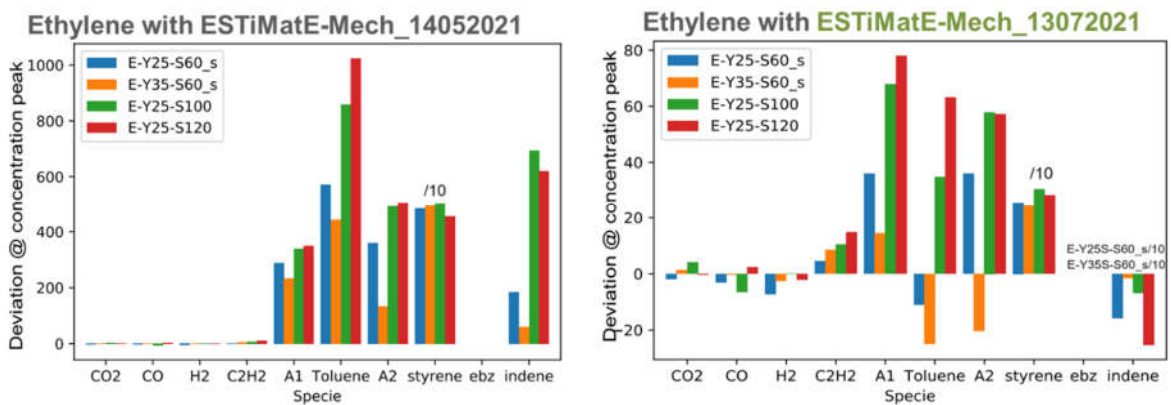
Fig. 13: Comparison between the concentrations peaks of different species predicted by the simulations with ESTiMatE-Mech_14052021 and ESTiMatE-Mech_13072021 and the ones obtained from the experimental data for four ethylene counterflow flames.

3.1   Iso-octane flames validation

In a similar way to the validation provided before for ethylene, a validation for six iso-octane flames was conducted. These flames are:

- I-Y35-S60: Y_F = 0.35, α_2 = 60 s^{-1}. Non-sooting flame
- I-Y47-S60_s: Y_F = 0.47, α_2 = 60 s^{-1}. Sooting flame
- I-Y50-S60_s: Y_F = 0.50, α_2 = 100 s^{-1}. Sooting flame
- I-Y60-S60_s: Y_F = 0.60, α_2 = 60 s^{-1}. Sooting flame
- I-Y60-S100: Y_F = 0.60, α_2 = 60 s^{-1}. Non-sooting flame
- I-Y60-S120: Y_F = 0.60, α_2 = 100 s^{-1}. Non-sooting flame

The modeling of the iso-octane flames was initially completed with the ESTiMatE-Mech_14052021. In this case a similar trend was observed that the one obtained with the ethylene flames. For iso-octane, a considerable overprediction of the PAHs was observed when modeling the counterflow flames with ESTiMatE-Mech_14052021. Similar to the case of the ethylene flames discussed before, a sensitivity analysis and rate of production analysis was carried out to evaluate the role of some reactions paths on the concentration profiles of the PAHs. These analyses allow to identify some reactions that were required to be modified or removed to have a better prediction of the PAHs. The modification of the reaction paths for the case of the iso-octane flames were also included in ESTiMatE-Mech_13072021.

Figure 14 presents that the prediction of the PAHs concentration profiles was considerable improved for all the iso-octane flames with ESTiMatE-Mech_13072021 when compared with the results with ESTiMatE-Mech_14052021
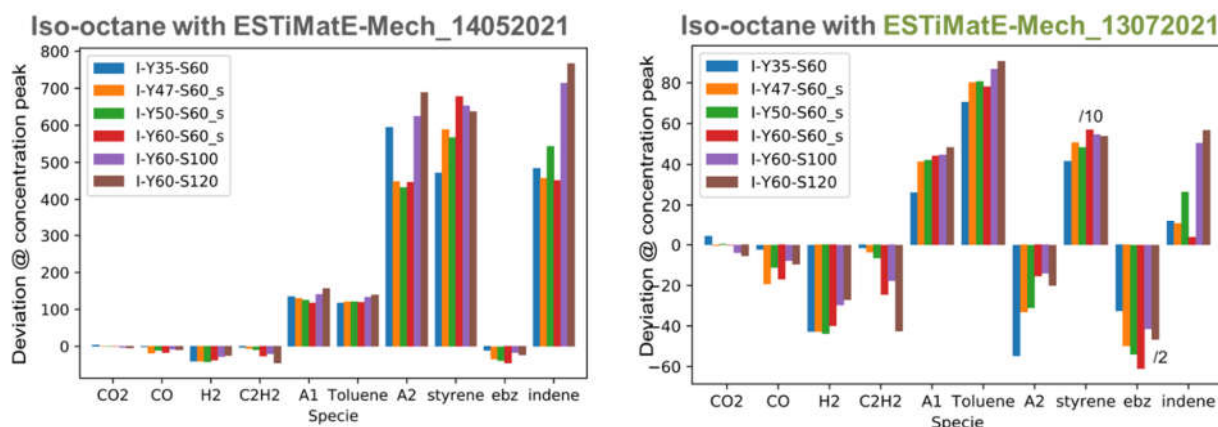
Fig. 14: Comparison between the concentrations peaks of different species predicted by the simulations with ESTiMatE-Mech_14052021 and ESTiMatE-Mech_13072021 and the ones obtained from the experimental data for six iso-octane counterflow flames.

## 3.3   Surrogate flames validation

The performance of the complete surrogate mechanism was analyzed by comparison of the modeling results with experimental species concentration profiles from: (i) two surrogate non-premixed counterflow (surrogate: n-dodecane 52%, iso-octane 15.8%,

cyclohexane 12.1% and 1,3,5-trimethylbenzene 20.2% in volumetric fraction). All the experimental flames at ambient pressure (1 bar) were provided by ESTiMatE partner KIT. These two flames are:

- S-Y45-S60_s: $Y_F = 0.35$, $\alpha_2 = 60$ s^{-1}. Sooting flame
- S-Y45-S90_s: $Y_F = 0.47$, $\alpha_2 = 60$ s^{-1}. Sooting flame

Figure 15 presents the validation of both flames with the last version of ESTiMatE-Mech (ESTiMatE-Mech_13072021) for the surrogate components and main species profiles. The reactivity of the four surrogate components is well predicted. Additionally, a good prediction of the main species concentration profiles (CO_2, CO, CH_4, H_2) is observed.
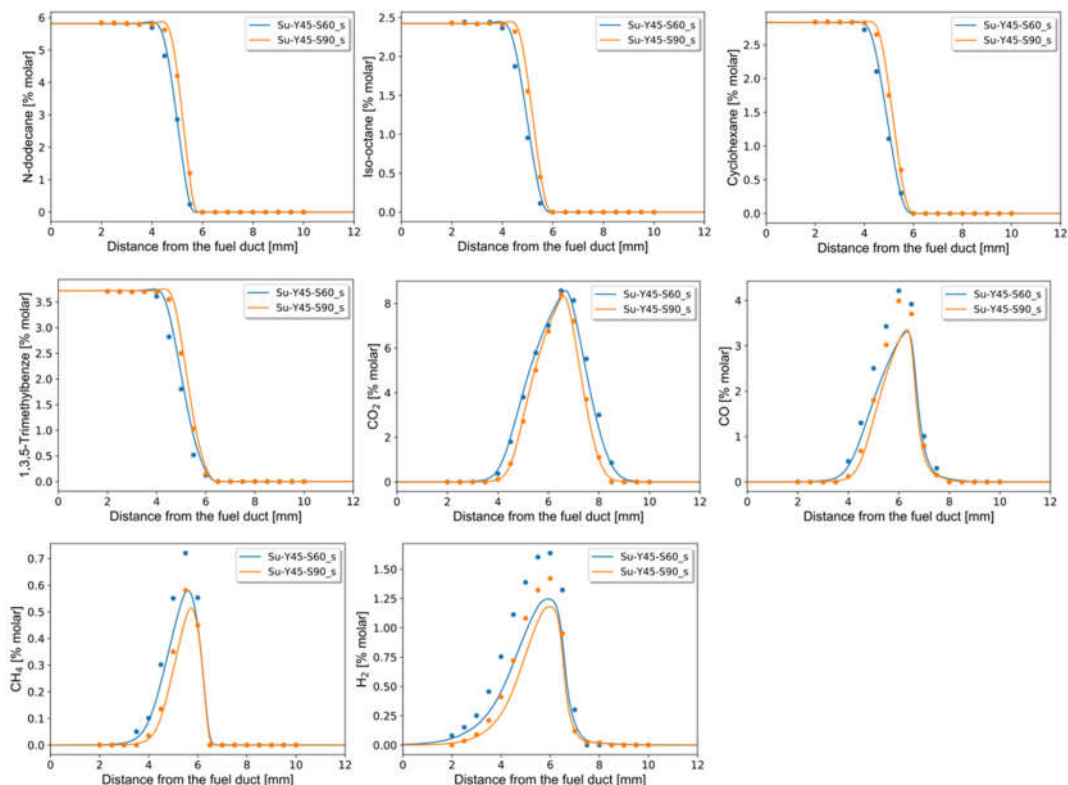
Fig. 15: Experimental (symbols) and numerical (curves) results obtained with ESTiMatE-Mech_1307 (EST-Mech_1307) of two surrogate counterflow flames. Experimental results of the four specie of the surrogate: n-dodecane, iso-octane, cyclohexane and 1,3,5-trimethylbenzene and some the main species profiles (CO_2, CO, CH_4 and H_2).

Figure 16 present the comparison between the modeling with ESTiMatE-Mech_1307 and the experimental data for some of the PAHs: A1 (benzene), toluene, A2 (naphthalene), byphenyl, A3 (phenanthrene) and A4 (pyrene). In the case of the PAHs, ESTiMatE-Mech_13072021 provides a good prediction of some of them: benzene (A1), and toluene. It is observed however a underprediction of larger PAHs such as Biphenyl, A2 (Naphthalene), A3 (phenanthrene) and A4 (pyrene). In this case, a preliminary analysis

allows to conclude that some reaction paths from 1,3,5-TMB that leads to the production of larger PAHS needs to be adapted (to account for the high contribution of 1,3,5-TMB to produce larger PAHs).
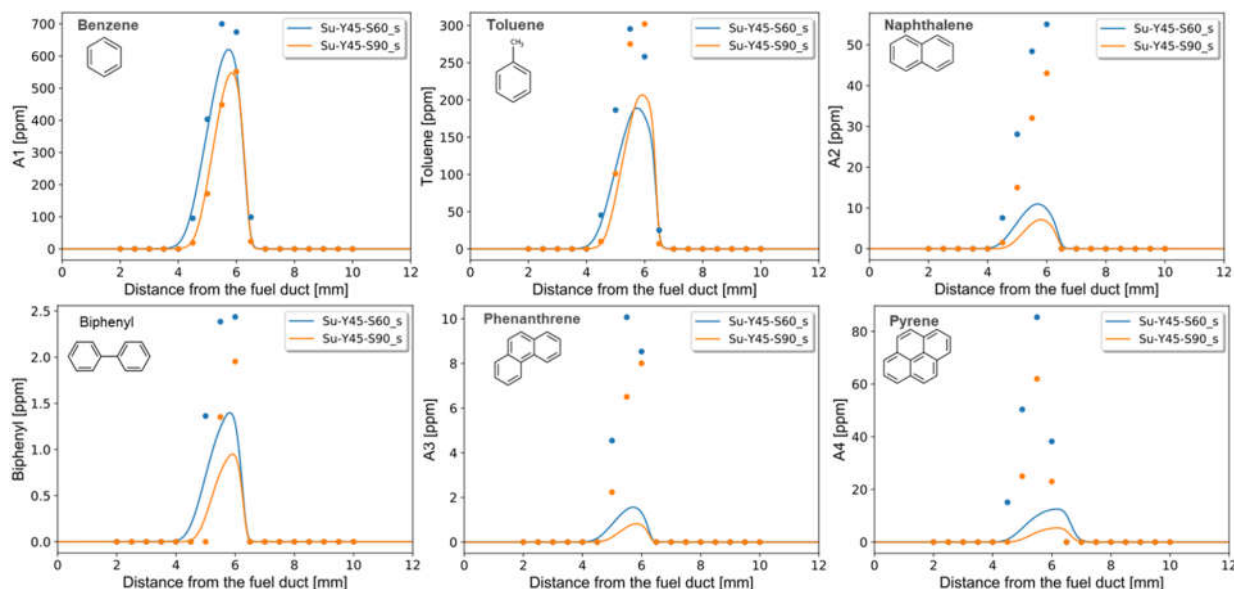
Fig. 16: Experimental (symbols) and numerical (curves) results obtained with ESTiMatE-Mech_1307 (EST-Mech_1307) of two surrogate counterflow flames. Experimental results of some of the PAHs precursors and PAHs.

4. ESTiMatE-Mech versions distributed to ESTiMatE partners

Table 2. ESTiMatE-Mech versions distributed to ESTiMatE partners

Name of the version	Main characteristics
ESTiMatE-Mech_14052021 214 species 1586 reactions	• All four surrogate components included: n-dodecane, iso-octane, cyclohexane, and 1,3,5-trimethylbenzene (1,3,5-TMB) as well as ethylene sub model • Good prediction of species reactivity and main species concentration profiles. • Prediction of the PAHs until A5 • Not accurate prediction of PAHs • Distributed to the ESTiMatE partners the 14/05/2021
ESTiMatE-Mech_13072021 214 species 1582 reactions	• Similar to ESTiMatE-Mech_14052021 but with good predictions of the PAHs • Distributed to the ESTiMatE partners the 13/07/2021

5. References

[1] Slavinskaya, N.A., Zizin, A., Aigner, M., 2010: "On Model Design of a Surrogate Fuel Formulation", J. Eng. Gas Turbines Power 132(11), 111501-111501-11.

[2] Kathrotia, T., Richter, S., Naumann, C., Slavinskaya, N., Methling, T., Braun-Unkhoff, M., Riedel, U., 2018: "Reaction Model Development for Synthetic Jet Fuels: Surrogate Fuels as a Flexible Tool to Predict Their Performance", Proc. ASME Turbo Expo 2018, GT2018-76997.

[3] Dooley, S., Won, S. H., Heyne, J., Farouk, T. I., Ju, Y., Dryer, F. L., Kumar, K., Hui, X.,et.al. 2012. "The experimental evaluation of a methodology for surrogate fuel formulation to emulate gas phase combustion kinetic phenomena", Comb. Flame 159(4), 1444 - 1466.

[4] Kim, D., Martz, J., & Violi, A. 2014. "A surrogate for emulating the physical and chemical properties of conventional jet fuel", Comb. Flame, 161(6), 1489 – 1498

[5] Honnet, S., Seshadri, K., Niemann, U., & Peters, N. 2009. "A surrogate fuel for kerosene", Proc. Combust. Inst., 32(1), 485 – 492

[6] Narayanaswamy, K., Pitsch, H., & Pepiot, P. 2016. "A component library framework for deriving kinetic mechanisms for multi-component fuel surrogates: Application for jet fuel surrogates", Comb. Flame 165, 288 - 309.

[7] Kathrotia, T., Oßwald, P., Naumann, C., Richter, S., Köhler, M., 2021: "Combustion kinetics of alternative jet fuels, Part-II: Reaction model for fuel surrogate", Fuel 302 (2021) 120736.

[8] Kathrotia, T., Oßwald, P., Zinsmeister, J., Methling; T., Köhler, M., 2021: "Combustion kinetics of alternative jet fuels, Part-III: Combustion kinetics of alternative jet fuels, Part-III: Fuel modeling and surrogate strategy", Fuel 302 (2021) 120737.

[9] Malewicki, T., Gudiyella, S., Brezinsky, K., 2013: "Experimental and modeling study on the oxidation of Jet A and the n-dodecane/iso-octane/n-propylbenzene/1,3,5-trimethylbenzene surrogate fuel", Comb. Flame 160(1), 17–30.

[10] Diévart, P., Kim, H.H., Won, S.H., Ju, Y., Dryer, F.L., Dooley, S., Wang, W., Oehlschlaeger, M.A., 2013: "The combustion properties of 1,3,5-trimethylbenzene and a kinetic model", Fuel 109, 125–136.

[11] Andrae, J.C.G., 2011: "A kinetic modeling study of self-ignition of low alkylbenzenes at engine-relevant conditions", Fuel Process. Technol. 92(10), 2030–2040

[12] Narayanaswamy, K., Blanquart, G., Pitsch, H., 2010: "A consistent chemical mechanism for oxidation of substituted aromatic species", Comb. Flame 157(10), 1879–1898.

[13] Ranzi, E., Frassoldati, A., Grana, R., Cuoci, A., Faravelli, T., Kelley, A.P., Law, C.K., 2012: "Hierarchical and comparative kinetic modeling of laminar flame speeds of hydrocarbon and oxygenated fuels", Prog. Energy Combust. Sci. 38(4), 468–501.

[14] Ranzi, E., Frassoldati, A., Stagni, A., Pelucchi, M., Cuoci, A., Faravelli, T., 2014: "Reduced Kinetic Schemes of Complex Reaction Systems: Fossil and Biomass-Derived Transportation Fuels", Intern. J. Chem. Kinet. 46(9), 512–542.

[15] Battin-Leclerc, F., Bounaceur, R., Belmekki, N., Glaude, P.A., 2006: "Experimental and modeling study of the oxidation of xylenes", Intern. J. Chem. Kinet. 38(4), 284–302.

[16] Shen, H.S., Oehlschlaeger, M.A., 2009: "The autoignition of C8H10 aromatics at moderate temperatures and elevated pressures", Comb. Flame 156(5), 1053–1062.

[17] Ji, C., Dames, E., Wang, H., Egolfopoulos, F.N., 2012: "Propagation and extinction of benzene and alkylated benzene flames", Comb. Flame 159(3), 1070–1081.

[18] Gaïl, S., Dagaut, P., 2007: "Oxidation of m-xylene in a jsr: Experimental study and detailed chemical kinetic modeling", Combust. Sci. Technol. 179(5), 813–844.

[19] Ramirez-Hernandez, A.Y., Kathrotia, T., Methling, T., Braun-Unkhoff, M., Riedel, U. Reaction Model Development of Selected Aromatics as Relevant Molecules of a

Kerosene Surrogate - The Importance of M-Xylene within the Combustion of 1,3,5-trimethylbenzene. J. Eng. Gas Turbines Power GTP-21-1384. Accepted Manuscript.

[20]   Gudiyella, S. and Brezinsky, K., High pressure study of 1,3,5-trimethylbenzene oxidation, Comb. Flame 159 (2012) 3264-3285.

[21]   Methling, T., Braun-Unkhoff, M., Riedel, U., A novel linear transformation model for the analysis and optimisation of chemical kinetics, Combust. Theor. Model. 21 (2017) 503-528.

[22]   Methling, T., Braun-Unkhoff, M., Riedel, U., An optimised chemical kinetic model for the combustion of fuel mixtures of syngas and natural gas, Fuel 262 (2020) 116611.

[23]   F. Rao, B. Li, P. Li, C. Zhang, X. Li, Shock-Tube Study of the Ignition of Gas-Phase 1,3,5-Trimethylbenzene in Air, Energy Fuels 28 (2014) 6707-6713.

[24]   X. Hui, A. K. Das, K. Kumar, C. Sung, S. Dooley, F. L. Dryer, Laminar flame speeds and extinction stretch rates of selected aromatic hydrocarbons, Fuel 97 (2012) 695-702.

[25]   D. Goodwin, H. Moffat, R. Speth, Cantera: An object-oriented software toolkit for chemical kinetics, thermodynamics, and transport processes, http://www.cantera.org, version 2.4.0.

Nomenclature

p	Pressure [Pa]
T	Temperature [K]
t	Time [s]
S_u	Laminar burning velocity [m/s]
Y_F	Fuel mass fraction
α_2	Global Strain rate at the oxidizer side [s^{-1}]

Greek letters

φ	Equivalence ratio
τ	Ignition delay time

Subscripts

ign	Ignition